THE JOURNAL OF PHYSICAL CHEMISTRY B LETTERS

**2007,** *111,* 13143−13146
Published on Web 10/25/2007



# Observation of Kinetic and Structural Scalings during Slow Coalescence of Nanobubbles in an Aqueous Solution

**Fan Jin,*,† Xiaodong Ye,‡ and Chi Wu†,‡**

*Department of Chemistry, The Chinese University of Hong Kong, Shatin, N.T., Hong Kong, and The Hefei National Laboratory of Physical Science at Microscale, Department of Chemical Physics, The University of Science and Technology of China, Hefei, Anhui 230026, China*

*Received: September 6, 2007; In Final Form: October 8, 2007*

The addition of salt can induce the slow coalescence of nanobubbles (~100 nm) in an aqueous solution of α-cyclodextrin (α-CD). A combination of static and dynamic laser light scattering was used to follow the coalescence. Our results reveal that its kinetic and structural properties follow some scaling laws; namely, the average size ($<\zeta>$) of the nanobubbles is related to their average mass ($<M>$) and the coalescence time ($t$) as $<M> \sim <\zeta>^{d_f}$ and $<\zeta> \sim t^{\gamma}$ with two salt-concentration-dependent scaling exponents ($d_f$ and $\gamma$). For a lower sodium chloride concentration ($C_{NaCl} = 40$ mM), $\gamma = 0.13 \pm 0.01$ and $d_f = 1.71 \pm 0.02$. The increase of $C_{NaCl}$ to 80 mM results in $\gamma = 0.32 \pm 0.01$ and $d_f = 1.99 \pm 0.01$. The whole process has two main stages: the aggregation and the coalescence. At the lower $C_{NaCl}$, the process essentially stops in the aggregation stage with some limited coalescence. At higher $C_{NaCl}$, coalescence occurs after the aggregation and results in large bubbles.

## Introduction

Generally speaking, nanobubbles in water are puzzling, capricious, and less understood. Most of previous experimental and theoretical studies were focused on a flat hydrophobic surface immersed in water or an aqueous solution.[1−5] Attard et al.[1,2,6,7] have made some significant contributions in this area. They have obtained the first image of nanobubbles on a hydrophobic surface by using tapping-mode AFM. They showed that some long-range (~100 nm) hydrophobic attraction exists between the two hydrophobic surfaces because of some previously existing bridging nanobubbles. In our recent studies, we found that small nanobubbles exist in different aqueous solutions, including surfactant/water, alcohol/water, sugar/water, and other water-soluble organic molecule solutions.[8] It should be noted that no stabilized "bare" nanobubbles was observed in our experiment, implying that the existence of small water-soluble organic molecules is essential to the existence of stable nanobubbles. Further study indicates that these nanobubbles have a negatively charged interface.[9] The electrostatic repulsion among different nanobubbles can be reduced by the addition of low-molar-mass electrolytes, similar to the salt-out effect in a typical aqueous colloidal dispersion. Therefore, the addition of salt can induce the nanobubble aggregation. The only difference is that aggregated nanobubbles are expected to further undergo a slow coalescence process.

Numerous experimental and theoretical studies have been devoted to the aggregation of colloidal particles in various dispersions in the past.[10−15] Depending on the sticking probability ($p_s$) between two colloidal particles, the process can be characterized as the diffusion-limited cluster−cluster aggregation (DLCA, $p_s \sim 100\%$) and the reaction-limited cluster−cluster aggregation (RLCA, $p_s \ll 100\%$).[16,17] One distinctive feature between DLCA and RLCA is their different scalings between the mass ($M$) and size ($R$) of the aggregates, that is, different fractal dimensions ($d_f$) in $M \sim R^{d_f}$. The DLCA leads to large aggregates with a more open and less uniform structure with $d_f \sim 1.7-1.9$ in a three-dimensional space. The kinetics of DLCA is described by $R \sim t^{\gamma}$ with $\gamma < 1$, and typically, $\gamma = 1/d_f$. Alternatively, $d_f$ in RLCA is in the range of 2.0−2.5 and $R \sim e^{bt}$, where $b$ is a constant, depending on the dispersion nature.[18]

The aggregation of hard colloidal particles and the coalescence of soft nanobubbles are different because small nanobubbles can merge into one large bubble. Note that such coalescence should depend on the interfacial properties of the nanobubbles. Unfortunately, the gas/water interface is less understood.[19,20] Therefore, a better understanding of the nanobubble coalescence is an important theoretical and practical problem. Its implications include the prevention of decompression sickness and the microboiling process.[21−23] A combination of different modern scattering techniques has provided a better opportunity to study the nanobubble coalescence over a wide range of observation lengths and times.

## Experiments

In the current study, we selected α-CD (GR) aqueous solutions because small nanobubbles (Radius ~80 nm) can spontaneously form and be stabilized by water-soluble α-CD molecules in the absence of salt.[8,9] We also estimate that the volume faction ($f$) of the nanobubble phase is in the range of $0.8 - 8 \times 10^{-4}$ and know that the nanobubble interface is

* Corresponding author. E-mail: toctutedi@cuhk.edu.hk. The Hong Kong address should be used for all correspondence.
† The Chinese University of Hong Kong.
‡ The University of Science and Technology of China.

10.1021/jp077190l CCC: $37.00 

negatively charged with a ζ potential of c.a. −40 mV. The most important fact is that such formed nanobubbles are stable in α-CD aqueous solutions over a long time. The addition of NaCl can make the nanobubbles unstable, especially when $C_{NaCl} >$ ~20 mM. A combination of static and dynamic laser light scattering (LLS) enables us to follow the nanobubble coalescence in situ in the solution ($C_{\alpha-CD} = 7.90 \times 10^{-3}$ g/mL) in the presence of different amounts of NaCl (~40−80 mM).

In dynamic LLS, we measured the coalescence time-dependent intensity−intensity time correlation function ($G^{(2)}(\tau)$). Our results reveal that each $G^{(2)}(\tau)$ from an aqueous solution with nanobubbles has two relaxation modes, which can be well fitted by a double exponential function.[8] The fast mode is related to individual α-CD molecules free in the solution, whereas the slow mode is attributed to small nanobubbles with α-CD molecules adsorbed at the gas/water interface of each nanobubble. Therefore, $[G^{(2)}(\tau) - B]/B$ can be expressed as[8,24]

$$\{[G^{(2)}(\tau) - B]/B\}^{1/2} = A_{fast}(\theta)\, e^{-<D_{fast}>q^2\tau} + A_{slow}(\theta)\, e^{-<D_{slow}>q^2\tau} \quad (1)$$

where $B$ is the measured baseline, $<D>$ is the average translational diffusion coefficient, $A(\theta)$ is the intensity contribution of each relaxation mode, $\theta$ is the scattering angle, and $q$ is the scattering vector that related the incident wave length ($\lambda_0$) and the refractive index ($n$) of scattering media as $q = 4\pi n/\lambda_0 \sin \theta/2$. Note that $A_{fast}(\theta) + A_{slow}(\theta) = 1$. By using a double exponential fit and the Stokes−Einstein equation, each measured $G^{(2)}(\tau)$ leads to two average dynamic correlation lengths, $<\zeta>_{D,fast}$ and $<\zeta>_{D,slow}$. The time-average scattering intensity from each mode can be calculated from the total time-averaged scattering intensity ($<I(\theta)>$) measured in static LLS and $A(\theta)$ from dynamic LLS; that is, $<I(\theta)>_{fast} = <I(\theta)>A_{fast}(\theta)$ and $<I(\theta)>_{slow} = <I(\theta)>A_{slow}(\theta)$. The plot of $1/<I(\theta)>_{fast}$ or $1/<I(\theta)>_{slow}$ versus $q^2$ leads to a static correlation length ($\zeta_{S,fast}$ or $\zeta_{S,slow}$) and the time-averaged scattering intensity at $q \rightarrow 0$ ($<I(0)>_{fast}$ or $<I(0)>_{slow}$) on the basis of[25]

$$<I(q)> = \frac{<I(0)>}{1 + q^2\zeta_S^{\,2}} \quad (2)$$

In this study, we concentrate on the time dependence of $<\zeta>_{D,slow}$, $<\zeta>_{S,slow}$, $<I(q)>_{slow}$ and $<I(0)>_{slow}$ as well as the angular dependence of $<I(q)>_{slow}$ during the nanobubble coalescence. The correlation-length dependence of $<I(q)>_{slow}$ or $<I(0)>_{slow}$ reveals structural information of the nanobubbles during the coalescence.

## Results and Discussion

Figure 1 shows both the average correlation length and the average scattering intensity of the nanobubbles' increase during the coalescence in the presence of two different amounts of salt. As expected, the coalescence becomes faster when more salts are added. Such kinetic behaviors are well described by $<I(q)>_{slow} \sim t^{\gamma(q)}$, $<I(0)>_{slow} \sim t^{\gamma(0)}$, $<\zeta>_{D,slow} \sim t^{\gamma_D}$ and $<\zeta>_{S,slow} \sim t^{\gamma_S}$. For $C_{NaCl} = 40$ mM, $\gamma(q) = 0.28 \pm 0.01$, $\gamma(0) = 0.33 \pm 0.01$, $\gamma_D = 0.13 \pm 0.01$, and $\gamma_S = 0.21 \pm 0.01$; for $C_{NaCl} = 80$ mM, $\gamma(q) = 0.65 \pm 0.01$, $\gamma(0) = 0.76 \pm 0.02$, $\gamma_D = 0.32 \pm 0.01$, and $\gamma_S = 0.37 \pm 0.01$. The scaling exponents clearly vary with the salt concentration. Note that $<I(20°)>$ in Figure 1b starts to decrease after ~3000 min. This is because the nanobubbles are too large (>~500 nm) to be stable in the solution.

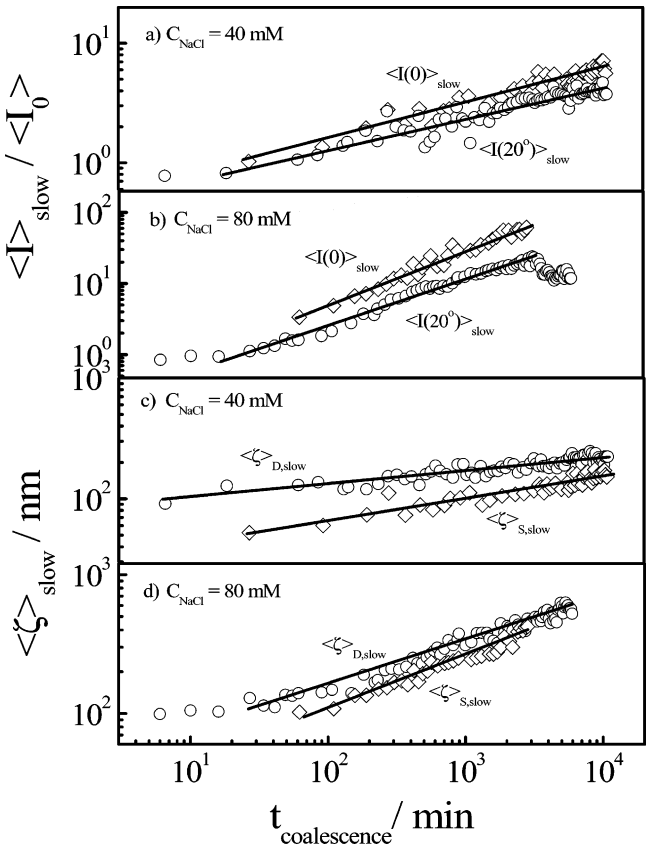


**Figure 1.** Time dependence of average scattering intensities ($<I>_{slow}$ at $\theta = 0$ and 20°) and average static and dynamic correlation lengths ($<\zeta>_{S,slow}$ and $<\zeta>_{D,slow}$) of nanobubbles in an α-CD aqueous solution, where lines represent fittings of different scaling equations and each slope leads to a scaling exponent.

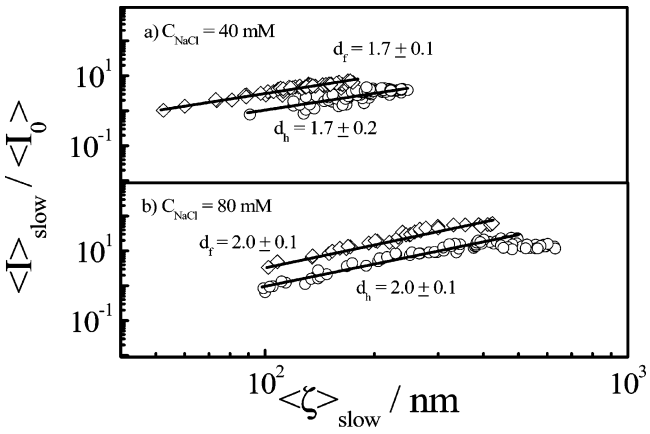


**Figure 2.** Correlation length ($<\zeta>_{slow}$) dependence of average scattering intensity ($<I>_{slow}$) of nanobubbles in an α-CD aqueous solution, where lines represents fittings of different scalings and each slope leads to a scaling exponent ($d_f$ or $d_h$).

Figures 2 and 3 reveal some scalings between different time-averaged scattering intensities and different correlation lengths or a dimensionless parameter, $q<\zeta>_{S,slow}$, in the range $q<\zeta>_{S,slow} > 1$; namely, $<I(0)>_{slow} \sim <\zeta>_{S,slow}^{d_f}$, $<I(q)>_{slow} \sim <\zeta>_{D,slow}^{d_h}$, and $<I(q)> \sim q^{-d_f}$, where $d_f$ and $d_h$ are the fractal and hydrodynamic dimensions, respectively.[11] For each given salt concentration, $d_f \approx d_h$, which is consistent with the DLCA theory.[12] The salt-concentration-dependent fractal dimension, that is, $d_f = 1.7 \pm 0.1$ for $C_{NaCl} = 40$ mM and $d_f = 2.0 \pm 0.1$ for $C_{NaCl} = 80$ mM, shows that the aggregation of small nanobubbles results in different structures. The smaller the $d_f$,

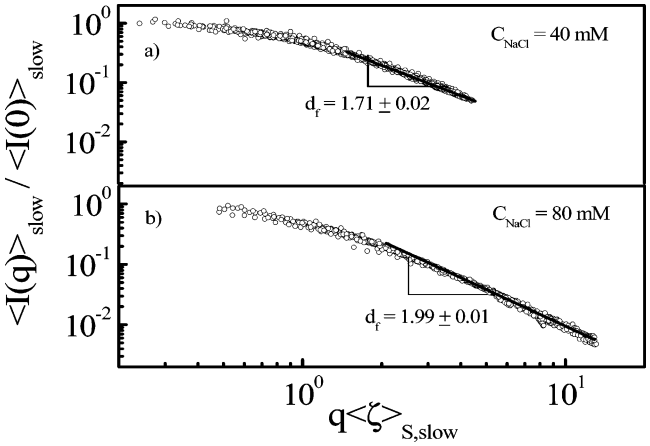


**Figure 3.** $q<\zeta>_{S,slow}$ dependence of normalized average scattering intensity ($<I(q)>_{slow}/<I(0)>_{slow}$) of nanobubbles in an α-CD aqueous solution, where lines represents fittings of different scalings in the range $q<\zeta>_{S,slow} > 1$ and each slope leads to a scaling exponent ($d_f$).

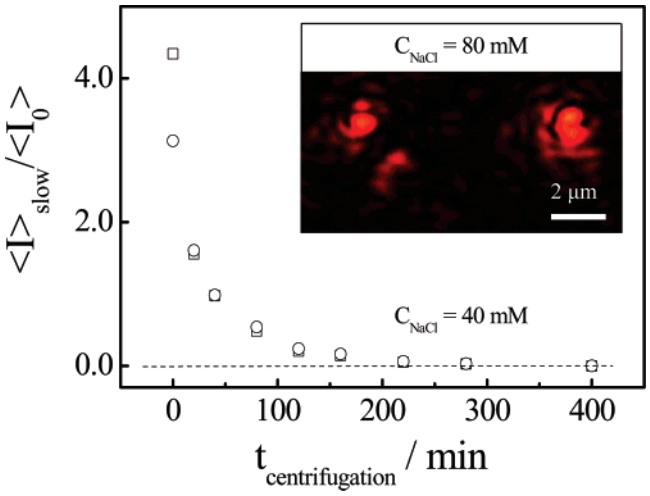


**Figure 4.** Centrifugation time dependence of average scattering intensity ($<I>_{slow}$) of nanobubbles in an α-CD aqueous solution, where □ and ○ represent top and bottom layers of solution. Before the centrifugation, the solution has been kept at 25 °C for ∼100 h after the addition of salt. The inset shows a photo of microbubbles taken by a LECICA optic microscope.

the looser the structure. Here, $d_f = 1.7$ indicates a classical DLCA process. Such a lower $d_f$ also implies no or rather limited coalescence of small nanobubbles. In other words, small nanobubbles only aggregate together. For $C_{NaCl} = 80$ mM, $d_f = 2.0$, reflecting a relatively denser structure. Presumably, the higher $d_f$ indicates that small nanobubbles coalesce into a larger bubble after they aggregate together.

For $C_{NaCl} = 40$ mM, both the averaged scattering intensity and the average correlation length continuously increase even after ∼100 h because of continuous coalescence. In a real experiment, large bubbles eventually float out of the solution. Note that after a sufficiently long time no nanobubbles can be observed in the presence of such a high amount of salt.[9] To confirm that the nanobubbles' phase has a lower density, we centrifuged the solution at 3000 rpm for a very short time to force lighter bubbles to float up. We found that the solution separated into two layers. The top layer scatters much more light than the bottom one. Figure 4 shows that as the centrifugation time increases (>∼20 min) $<I>_{slow}$ decreases and the difference between the two layers disappears. Finally, (>∼300 min) no nanobubbles can be detected in the solution ($<I>_{slow} \rightarrow 0$). Figure 5 shows a better view of the disappearance of the

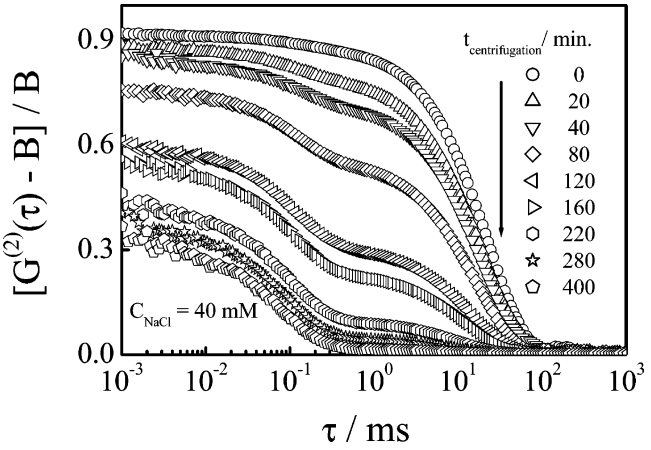


**Figure 5.** Centrifugation time dependence of normalized intensity−intensity time correlation function $[G^{(2)}(\tau) - B]/B$ of an α-CD aqueous solution.

nanobubbles (the slow mode). For $C_{NaCl} = 80$ mM, the average size of the nanobubbles is ∼600 nm after ∼100 h so that some larger bubbles (>1 μm) become visible even in an optical microscope, as shown in the inset of Figure 4.

## Conclusions

In summary, the addition of salt, such as NaCl, induces slow aggregation and coalescence of small nanobubbles in an aqueous solution. We have, *for the first time*, observed some scaling laws between the average size and the coalescence time or the average mass of large nanobubble aggregates. Such scalings are different from classical diffusion-limited cluster−cluster aggregation (DLCA); namely, the scaling exponent varies with the salt concentration and the measured fractal dimension ($d_f$) is over the range (1.7−1.9) of a DLCA process limited. Our results indicate that in the presence of high amount of salt the aggregation of small nanobubbles leads to a denser structure, presumably because of the coalescence of nanobubbles because salt affects the gas/water interface of each nanobubble.

**Acknowledgment.** The financial support of the Chinese Academy of Sciences (CAS) Special Grant (KJCX2-SW-H14), the National Natural Scientific Foundation of China (NNSFC) Projects (20534020 and 20574065), and the Hong Kong Special Administration Region (HKSAR) Earmarked Project (CU-HK4036/05P, 2160269) is gratefully acknowledged.

## References and Notes

(1) Tyrrell, J. W. G.; Attard, P. *Phys. Rev. Lett.* **2001**, *87*, 176104−1.
(2) Papker, J. L.; Claesson, P. M.; Attard, P. *J. Phys. Chem.* **1994**, *98*, 8468.
(3) Agrawal, A.; Park, J.; Ryu, D.; Hammond, Y. P. T.; Russell, T. P.; McKinley, G. H. *Nano Lett.* **2005**, *5*, 1751.
(4) Zhang, X. H.; Zhang, X. D.; Lou, S. T.; Zhang, Z. X.; Sun, J. L.; Hu, J. *Langmuir* **2004**, *20*, 3813.
(5) Yang, J.; Duan, J.; Fornasiero, D.; Ralston, J. *J. Phys. Chem. B* **2003**, *107*, 6139.
(6) Attard, P. *J. Chem. Phys.* **1989**, *93*, 6441.
(7) Carambassis, A.; Jonker, L. C.; Attard, P.; Rutland, M. W. *Phys. Rev. Lett.* **1998**, *80*, 5357.
(8) Jin, F.; Ye, J.; Hong, L.; Lam, H.; Wu, C. *J. Phys. Chem. B* **2007**, *111*, 2255.
(9) Jin, F.; Li, J. F.; Ye, X. D.; Wu, C. *J. Phys. Chem. B* **2007**, *111*, 11745.
(10) Zhou, Z.; Chu, B. *J. Colloid Interface Sci.* **1991**, *143*, 356.
(11) Lin, M. Y.; Lindsay, H. M.; Weitz, D. A.; Ball, R. C.; Klein, R.; Meakin, P. *Nature* **1989**, *40*, 4665 and the references therein.
(12) Micali, N.; Mallamace, F.; Romeo, A.; Purrello, R.; Scolaro, L. *J. Phys. Chem. B* **2000**, *104*, 5897 and the references therein.
(13) Martin, J. E.; Ackerson, B. *J. Phys. Rev. A* **1985**, *31*, 1180.

(14) Jullien, R.; Botet, R.; Mors, P. M. *Faraday Discuss.* **1987**, *83*, 125.
(15) Reinecke, H.; Fazel, N.; Dosiere, M.; Guenet, J. M. *Macromolecules* **1997**, *30*, 8360.
(16) Botet, R.; Kolb, M.; Jullien, R. In *Physics of Finely Divided Matter*; Boccara, N., Daoud, M., Eds.; Springer-Verlag: New York, 1985.
(17) Mandlbrot, B. J. *Fractals, Form and Dimensions*; Freeman: San Francisco, CA, 1977.
(18) Weitz, D. A.; Huang, J. S.; Lin, M. Y.; Sung, J. *Phys. Rev. Lett.* **1985**, *54*, 1416.
(19) Jungwirth, P.; Tobias, D. J. *Chem. Rev.* **2006**, *106*, 1259.
(20) Shen, Y. R.; Ostroverkhov, V. *Chem. Rev.* **2006**, *106*, 1140.
(21) Craig, V. S. J.; Ninham, B. W.; Pashley, R. M. *J. Phys. Chem.* **1993**, *97*, 10192.
(22) Craig, V. S. J.; Ninham, B. W.; Pashley, R. M. *Nature* **1993**, *364*, 317.
(23) Hills, B. A. A *Thermodynamic and Kinetic Approach to Decompression Sickness*; Libraries Board of S. A.: Adelaide, Australia, 1966.
(24) Berne, B.; Pecora, R. *Dynamic Light Scattering*; Plenum Press: New York, 1976.
(25) Chu, B. *Laser Light Scattering*, 2nd ed.; Academic Press: New York, 1991.